Ablation of triadin causes loss of cardiac Ca^{2+} release units, impaired excitation–contraction coupling, and cardiac arrhythmias

Nagesh Chopra[a,1], Tao Yang[a,1], Parisa Asghari[b], Edwin D. Moore[b], Sabine Huke[a], Brandy Akin[c], Robert A. Cattolica[d], Claudio F. Perez[e], Thinn Hlaing[a,2], Barbara E. C. Knollmann-Ritschel[f], Larry R. Jones[c], Isaac N. Pessah[d], Paul D. Allen[e], Clara Franzini-Armstrong[g,3], and Björn C. Knollmann[a,3]

[a]Division of Clinical Pharmacology, Departments of Medicine and Pharmacology, Vanderbilt University, Nashville, TN 37232; [b]Department of Cellular and Physiological Sciences, Life Sciences Institute, University of British Columbia, Vancouver, BC, Canada V6T 1Z3; [c]Department of Medicine, Krannert Institute of Cardiology, Indiana University, Indianapolis, IN 46202; [d]Department of Molecular Biosciences, School of Veterinary Medicine, University of California, Davis, CA 95616; [e]Department of Anesthesia, Perioperative, and Pain Medicine, Brigham and Women's Hospital, Boston, MA 02115; [f]Department of Pathology, Uniformed Services University of the Health Sciences, Bethesda, MD 20814; and [g]Department of Cell and Developmental Biology, University of Pennsylvania, Philadelphia, PA 19104

Contributed by Clara Franzini-Armstrong, March 18, 2009 (sent for review December 3, 2008)

Heart muscle excitation–contraction (E-C) coupling is governed by Ca^{2+} release units (CRUs) whereby Ca^{2+} influx via L-type Ca^{2+} channels (Cav1.2) triggers Ca^{2+} release from juxtaposed Ca^{2+} release channels (RyR2) located in junctional sarcoplasmic reticulum (jSR). Although studies suggest that the jSR protein triadin anchors cardiac calsequestrin (Casq2) to RyR2, its contribution to E-C coupling remains unclear. Here, we identify the role of triadin using mice with ablation of the *Trdn* gene (*Trdn*$^{-/-}$). The structure and protein composition of the cardiac CRU is significantly altered in *Trdn*$^{-/-}$ hearts. jSR proteins (RyR2, Casq2, junctin, and junctophilin 1 and 2) are significantly reduced in *Trdn*$^{-/-}$ hearts, whereas Cav1.2 and SERCA2a remain unchanged. Electron microscopy shows fragmentation and an overall 50% reduction in the contacts between jSR and T-tubules. Immunolabeling experiments show reduced colocalization of Cav1.2 with RyR2 and substantial Casq2 labeling outside of the jSR in *Trdn*$^{-/-}$ myocytes. CRU function is impaired in *Trdn*$^{-/-}$ myocytes, with reduced SR Ca^{2+} release and impaired negative feedback of SR Ca^{2+} release on Cav1.2 Ca^{2+} currents (I_{Ca}). Uninhibited Ca^{2+} influx via I_{Ca} likely contributes to Ca^{2+} overload and results in spontaneous SR Ca^{2+} releases upon β-adrenergic receptor stimulation with isoproterenol in *Trdn*$^{-/-}$ myocytes, and ventricular arrhythmias in *Trdn*$^{-/-}$ mice. We conclude that triadin is critically important for maintaining the structural and functional integrity of the cardiac CRU; triadin loss and the resulting alterations in CRU structure and protein composition impairs E-C coupling and renders hearts susceptible to ventricular arrhythmias.

cardiac muscle | sarcoplasmic reticulum | calsequestrin | Cav1.2 | RyR2

The cardiac Ca^{2+} release unit (CRU) is a multiprotein complex whose principle components include L-type Ca^{2+} channels (Cav1.2) juxtaposed to ryanodine receptor Ca^{2+} release channels (RyR2) (1). In cardiac excitation–contraction (E-C) coupling, Ca^{2+} current (I_{Ca}) via Cav1.2 triggers sarcoplasmic reticulum (SR) Ca^{2+} release through RyR2 release channels, a process that is highly regulated by RyR2-associated proteins and RyR2 phosphorylation (2). Among the CRU proteins, RyR2, triadin, junctin, and cardiac calsequestrin (Casq2) form a protein complex located in the junctional elements of the sarcoplasmic reticulum (jSR) (3). Triadin is encoded by the *Trdn* gene (4), which produces several isomeric forms that differ in size (5). Among these, the triadin-1 isoform is predominant in cardiac muscle (6). Triadin-1 has a membrane-spanning domain, a short cytoplasmic N-terminal segment, and a long, positively charged C-terminal domain extending into the lumen of the SR, which also contains the putative binding domain for Casq2 (6).

Although the function of cardiac triadin-1 is not explicitly known, attempts have been made to understand its physiologic role in cardiac muscle using acute adenoviral (7) and transgenic overexpression (8) and by reconstitution experiments in lipid bilayers (9). Changes in expression of triadin-1 are frequently accompanied by altered expression of its binding partners RyR2 (10), Casq2 (11), and junctin (10). The trimeric complex of Casq2, triadin-1, and junctin is thought to regulate SR Ca^{2+} release (9, 12). Deletion (11) or even modest reductions (13) in Casq2 protein increases diastolic SR Ca^{2+} leak and causes spontaneous SR Ca^{2+} release (SCR) and catecholaminergic cardiac arrhythmia. Deletion of junctin enhances SR Ca^{2+} cycling and contractility but is associated with delayed afterdepolarization–induced ventricular arrhythmias and premature death under conditions of physiologic stress (14).

To better understand the physiologic role of triadin-1 in the mammalian heart, we performed a comprehensive structural and functional evaluation of the *pan* triadin null (*Trdn*$^{-/-}$) mouse model. We found that triadin-1 is critically important to maintain the structural and functional integrity of the cardiac CRU, which is pivotal for both E-C coupling and maintaining a regular heart rhythm in mammalian hearts.

Results

Triadin-1 Deletion Reduces Expression of jSR Proteins. The generation of *Trdn*$^{-/-}$ mice and characterization of their skeletal muscle phenotype has been described previously (15). Here we report the cardiac phenotype of *Trdn*$^{-/-}$ mice. As expected (6), the immunoreactive 35/40-kDa doublet corresponding to the unglycosylated and glycosylated triadin-1 is absent in *Trdn*$^{-/-}$ microsomes (Fig. 1*A*). A 92-kDa immunoreactive protein, tentatively identified as the putative triadin-3 (6), was also present in *Trdn*$^{-/-}$ microsomes, further challenging the identity of this immunoreactive band as a *Trdn*-related protein (ref. 16 and Fig. 1*A*). Thus, on the basis of our data the 92-kDa band represents

Author contributions: E.D.M., I.N.P., P.D.A., C.F.-A., and B.C.K. designed research; N.C., T.Y., P.A., E.D.M., S.H., B.A., R.A.C., C.F.P., T.H., B.E.C.K.-R., L.R.J., C.F.-A., and B.C.K. performed research; C.F.P. and P.D.A. contributed new reagents/analytic tools; N.C., T.Y., P.A., E.D.M., S.H., B.A., R.A.C., C.F.P., T.H., B.E.C.K.-R., L.R.J., C.F.-A., and B.C.K. analyzed data; and N.C., E.D.M., L.R.J., I.N.P., P.D.A., C.F.-A., and B.C.K. wrote the paper.

The authors declare no conflict of interest.

[1]N.C. and T.Y contributed equally to this article.

[2]Present address: Department of Medicine, University of Miami, Miami, FL 33136.

[3]To whom correspondence may be addressed. E-mail: bjorn.knollmann@vanderbilt.edu or armstroc@mail.med.upenn.edu.

This article contains supporting information online at www.pnas.org/cgi/content/full/0902919106/DCSupplemental.

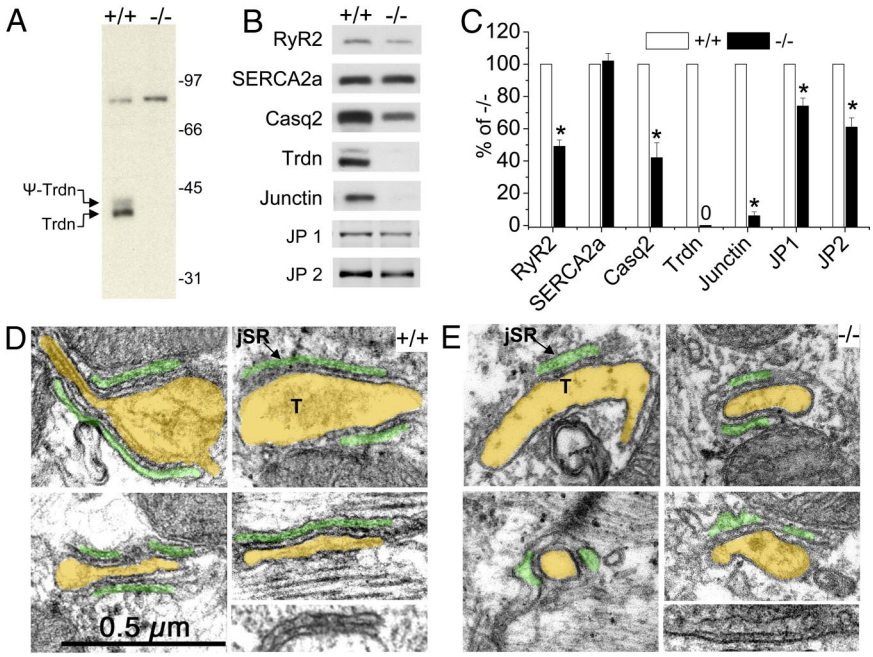

Fig. 1. Gene-targeted ablation of triadin reduces expression of jSR proteins and the extent of T-tubule jSR interfaces of cardiac CRUs. (*A*) Immunoblot of pooled microsomal preparations from *Trdn*$^{+/+}$ and *Trdn*$^{-/-}$ hearts. The 35/40-kDa double band represents triadin-1 and its glycosylated form, the only triadin isoform significantly expressed in adult mouse heart. The band at 92 kDa is a nonspecific cross-reacting band unrelated to triadin. (*B* and *C*) Representative examples of immunoblots of whole-heart homogenates (*B*) and summarized data (*C*) demonstrate reduced expression of jSR proteins in *Trdn*$^{-/-}$ (−/−) mice. $n = 5$ hearts per group. *, $P < 0.05$. (*D* and *E*) Electron micrographs from thin sections of age-matched *Trdn*$^{+/+}$ (*D*) and *Trdn*$^{-/-}$ (*E*) myocardium from the left ventricle showing details of dyads. For ease of identification, a transparent yellow overlay covers the lumen of T-tubules (T) and a green overlay that of the jSR domains. Structural details are visible under the overlay. A narrow cleft containing profiles of ''feet'' representing the cytoplasmic domains of RyR2 occupy the narrow junctional gap. The images were selected to illustrate 2 major differences between +/+ and −/− myocytes: The junctional SR domains of −/− myocytes are less extensive and have an increased width. Not shown is the result that jSR profiles are also less frequent in −/− myocytes. The combination of less-frequent and smaller contact areas results in a decrease of approximately 50% in areas occupied by RyR2 (see Table 1).

nonspecific binding of the antibody, and triadin-1 is the only triadin isoform that is detectable in murine myocardium.

SR proteins located in the jSR cisternae (RyR2, Casq2, junctin, and junctophilin 1 and 2) were all significantly decreased in *Trdn*$^{-/-}$ hearts (Fig. 1 *B* and *C*). Expression levels of the SR Ca^{2+} uptake pump, SERCA2a (Fig. 1 *B* and *C*) and phospholamban (data not shown) located in the free SR domain were not changed. Consistent with the reduction of RyR2 protein (Fig. 1*B*), B_{max} for high affinity [^{3}H]ryanodine binding sites was significantly reduced (*Trdn*$^{+/+}$: 570 ± 30 fmol/mg, $n = 6$; *Trdn*$^{-/-}$: 430 ± 25 fmol/mg, $n = 4$; $P = 0.0013$) in *Trdn*$^{-/-}$ preparations compared with *Trdn*$^{+/+}$ [supporting information (SI) Fig. S1]. When [^{3}H]ryanodine binding studies were repeated in a buffer containing high salt (1 M KCl) to optimize RyR2 binding, the B_{max} measured in *Trdn*$^{-/-}$ cardiac muscle was reduced by 42% compared with *Trdn*$^{+/+}$ (data not shown). In contrast, B_{max} of [^{3}H]PN200–110 binding, which binds with high affinity to Cav1.2, was not different between the 2 groups (Fig. S1). The K_D of neither radioligand was altered due to triadin-1 deletion. Thus, triadin-1 deletion caused significant reductions in RyR2 and associated jSR proteins without significant change in Cav1.2 expression in the plasma membrane.

Loss of Triadin-1 Alters the Architecture of Cardiac CRUs. In mammalian myocardium, RyR2, Casq2, triadin, junctin, and junctophilin are all located in terminal SR cisternae, where the jSR comes in close contact with either the plasma membrane (peripheral coupling) or the T-tubules (dyads), at the level of Z-lines. Together with juxtaposed Cav1.2 channels in the plasmalemma, jSR cisternae form the cardiac CRU.

Analysis of electron micrographs demonstrates that jSR cisternae were less frequent and had shorter RyR2-bearing junctional contacts with T-tubules (Fig. 1 *D* and *E* and Table 1). Overall, the reduced number and shorter contacts resulted in ≈56% reduction in total extent of RyR2-bearing jSR cisternae (Table 1), in good agreement with the 50% reduction in RyR2 protein measured by Western blot (Fig. 1*C*). At the same time, the remaining jSR cisternae were more variable in width and significantly wider in *Trdn*$^{-/-}$ hearts (Fig. 1*E* and Table 1). Casq2 was visible in the form of small condensed nodules in *Trdn*$^{+/+}$ (Fig. 1*D*) but was barely noticeable, showing only as a

Table 1. Quantitative electron microscopic morphometry of ventricular cardiac myocytes

Genotype	1. jSR lumen width (nm)	2. jSR contact length (nm)	3. jSR contacts per IMS	4. jSR extent (arbitrary units)
Trdn$^{+/+}$	21.7 ± 6.3 (179)	227 ± 142 (108)	0.42 ± 0.20 (85)	95 ± 28
Trdn$^{-/-}$	37.1 ± 15.0* (192)	139 ± 62* (82)	0.30 ± 0.22* (89)	42 ± 13*

jSR lumen width was significantly larger and more variable in *Trdn*$^{-/-}$ cells (see also Fig. 1 *C and D*). jSR extent (where feet are located) was obtained by multiplying the jSR contact length (column 2) by the frequency of dyads (= jSR contacts per intermyofibrillar space (IMS), column 3). jSR extent was reduced by 56% in the *Trdn*$^{-/-}$ myocardium. Data are mean ± SD. All data are from 3 mice. In parenthesis are the number of dyads (columns 1 and 2) and number of images (column 3). *, $P < 0.001$, Student's *t* test.

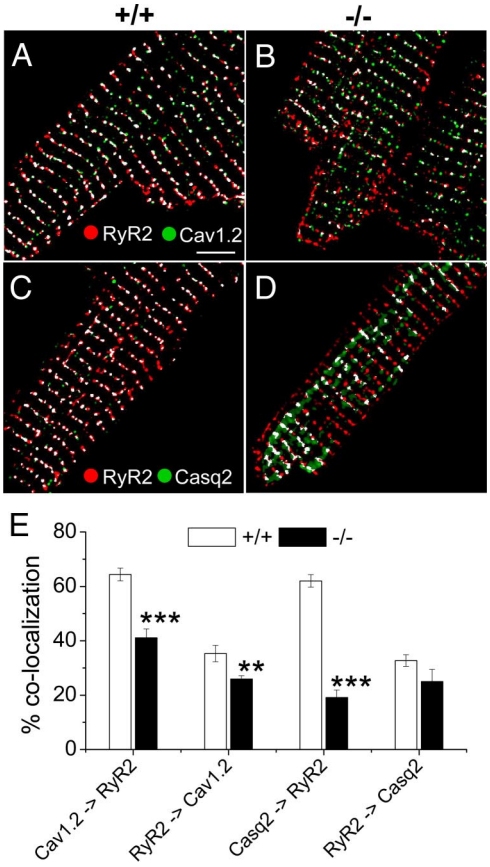

Fig. 2. Gene-targeted ablation of triadin increases localization of Cav1.2 and Casq2 in subcellular areas outside RyR2-containing dyads. (*A–D*) Isolated ventricular myocytes from +/+ (*A* and *C*) and −/− (*B* and *D*) were colabeled with antibodies against RyR2 (red) and either Cav1.2 (green; *A* and *B*) or Casq2 (green; *C* and *D*). White pixels indicate colocalization. (Scale bar, 5 μm.) (*E*) Colocalization of Cav1.2 and Casq2 with RyR2 is significantly reduced in −/− myocytes, demonstrating that a significant number of Cav1.2 and Casq2 are located outside the dyads. Data are mean ± SEM. ***, $P < 0.001$; **, $P < 0.01$; +/+ $n = 5$ myocytes; −/− $n = 6$ myocytes.

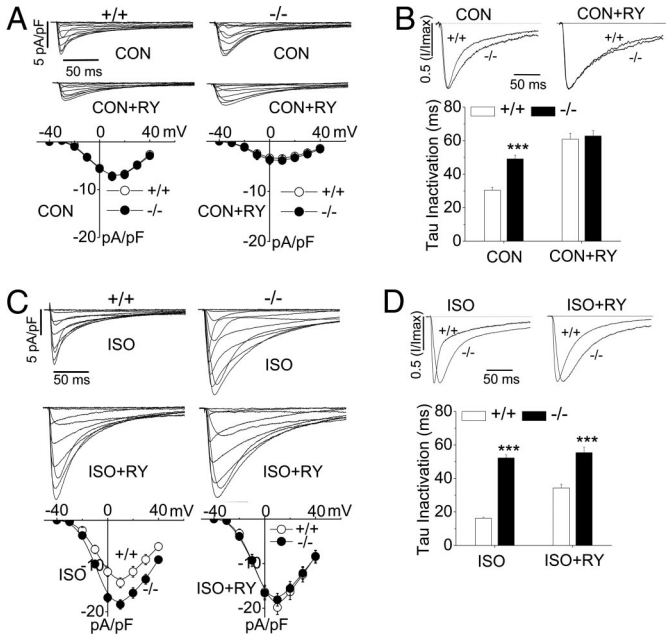

Fig. 3. *Trdn*$^{-/-}$ myocytes exhibit impaired Ca^{2+}-dependent inactivation of L-type Ca^{2+} current. (*A*) (*Top*) Representative examples of L-type Ca^{2+} currents (I_{Ca}) recorded from *Trdn*$^{+/+}$ (+/+) and *Trdn*$^{-/-}$ (−/−) myocytes in control conditions (CON) and in presence of 10 μM ryanodine (RY). (*Bottom*) Average current–voltage relationships. Myocyte size estimated by cell capacitance was not significantly different (+/+ 152 ± 4.3 pF; −/− 154 ± 3.7 pF; $n = 20$ each; $P = 0.73$). (*B*) Representative examples of superimposed normalized I_{Ca} records at 0 mV (*Left*) and averaged data (*Right*) in control conditions. Note that block of RyR2 channels with ryanodine abolished the differences in I_{Ca} inactivation. (*C*) I_{Ca} recordings in the presence of 1 μM ISO. −/− myocytes exhibit significantly larger I_{Ca} amplitudes. Note that ryanodine abolished the differences between +/+ and −/− myocytes. (*D*) I_{Ca} inactivation in ISO-stimulated myocytes. Although ryanodine reduced the differences between the 2 groups, I_{Ca} inactivation remained significantly slower in *Trdn-/-* myocytes even in the presence of RY. $n = 7$–10 myocytes from 3–4 different mice per genotype; ***, $P < 0.001$ vs. +/+.

diffuse density, in the *Trdn*$^{-/-}$ jSR (Fig. 1*E*). There was no significant widening of the free SR elements and no change in total SR volume (data not shown).

We next examined whether loss of triadin-1 also changes the relative positioning of 3 key CRU proteins. Immunolabeling of isolated ventricular myocytes from *Trdn*$^{+/+}$ mice with anti-RyR2 antibody (red) and anti-Cav1.2 antibody (green) shows well-defined and colocalized (white) foci located at the Z-lines corresponding to dyads (Fig. 2*A*). In *Trdn*$^{-/-}$ myocytes, the degree of colocalization of Cav1.2 with RyR2 was significantly reduced (Fig. 2 *B* and *E*). The non-colocalized Cav1.2 are part of either CRUs with reduced RyR2 content or nonfunctional CRUs lacking RyR2. Immunolabeling with anti-RyR2 and anti-Casq2 antibodies shows the dyadic colocalization of both proteins in *Trdn*$^{+/+}$ myocytes (Fig. 2*C*). The degree of colocalization of RyR2 with Casq2 was not significantly different in *Trdn*$^{-/-}$ myocytes, but colocalization of Casq2 with RyR2 was significantly reduced (Fig. 2 *D* and *E*). These data demonstrate that although some Casq2 protein is retained in jSR cisternae, a significant fraction of the Casq2 protein moves into longitudinal SR.

Triadin-1 Deletion Impairs Cardiac E-C Coupling. For cardiac E-C coupling, I_{Ca} through Cav1.2 is required to trigger Ca^{2+} release (17). As would be predicted by our ligand-binding studies (Fig. S1), I_{Ca} amplitude was not significantly different in *Trdn*$^{-/-}$ compared with *Trdn*$^{+/+}$ myocytes under control conditions (Fig. 3*A*). However, I_{Ca} inactivation was significantly slower in *Trdn*$^{-/-}$ myocytes (Fig. 3*B*). I_{Ca} inactivation is both voltage and Ca^{2+} dependent (18). Because of the close proximity of RyR2 and Cav1.2 in the dyad, Ca^{2+} released from the SR mediates a large fraction of Ca^{2+}-dependent I_{Ca} inactivation (19). Given that there are fewer RyR2 channels in *Trdn*$^{-/-}$ hearts (Fig. 1*B* and Fig. S1), a substantial fraction of Cav1.2 channels are not associated with RyR2 (Fig. 2*E*), and the differences in I_{ca} inactivation could be the result of impaired negative feedback on I_{ca} from SR Ca^{2+} release. Consistent with this idea, preventing SR Ca^{2+} release by blocking RyR2 channels with ryanodine abolished the differences in I_{ca} inactivation (Fig. 3*B*). Incubating myocytes for 30 min with 2 μM thapsigargin, which empties SR Ca^{2+} stores by blocking SR Ca^{2+} uptake, also abolished the differences in I_{Ca} inactivation time constants [*tau* at 0 mV (ms): *Trdn*$^{+/+}$: 62 ± 2.36, $n = 9$ vs. *Trdn*$^{-/-}$: 65.21 ± 2.57, $n = 12$; $P = 0.36$).

In ventricular myocytes, β-adrenergic receptor stimulation with isoproterenol (ISO) significantly increases I_{Ca} amplitude and accelerates I_{Ca} inactivation, in part by increasing the SR Ca^{2+} content and release (ref. 19 and Fig. 3*C*, *Left*). Ryanodine pretreatment further enhances I_{Ca} peak current amplitude in ISO-stimulated *Trdn*$^{+/+}$ myocytes, because large SR Ca^{2+} releases can curtail peak I_{Ca} (ref. 20 and Fig. 3*C*, *Left*). In *Trdn*$^{-/-}$ myocytes, ISO caused a greater percentage increase in I_{Ca} amplitude (Fig. 3*C*) than in *Trdn*$^{+/+}$ myocytes, which was accompanied by very slow I_{Ca} inactivation (Fig. 3 *C* and *D*).

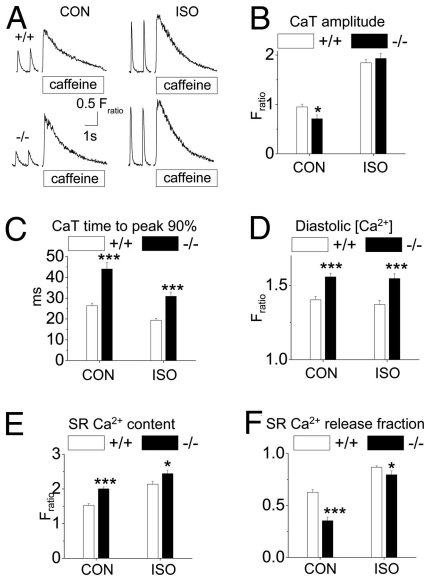

Fig. 4. *Trdn*$^{-/-}$ myocytes display impaired SR Ca^{2+} release despite increased SR Ca^{2+} content. (*A*) Representative examples of rapid caffeine (10 mM) application to *Trdn*$^{+/+}$ (+/+) and *Trdn*$^{-/-}$ (−/−) myocytes that were field stimulated at 1 Hz to maintain consistent SR Ca^{2+} load. The 2 last paced Ca^{2+} transients (CaT) are also shown. The amplitude of the caffeine transient was used as a measure of total SR Ca^{2+} content. Experiments were carried out in control conditions (CON) and in the presence of 1 μM ISO. (*B–F*) Comparisons of average CaT amplitudes (*B*), CaT rise time (0 to 90% of peak) (*C*), end-diastolic [Ca^{2+}] (*D*), SR Ca^{2+} content (*E*), and SR Ca^{2+} release fraction (*F*) in the 2 groups. *Trdn*$^{+/+}$ (+/+): $n = 37$ (CON) and 31 (ISO); *Trdn*$^{-/-}$ (−/−): $n = 38$ (CON) and 23 (ISO); *, $P < 0.05$; ***, $P < 0.001$. CaT time to peak 90%, time to reach 90% of peak CaT height.

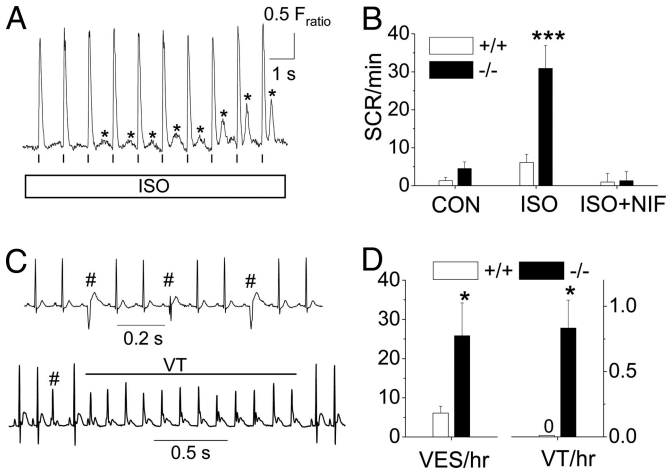

Fig. 5. Catecholamine challenge with ISO caused premature SCR in *Trdn*$^{-/-}$ myocytes and ventricular ectopy in *Trdn*$^{-/-}$ mice. (*A*) Representative examples of premature SCR (*) in a *Trdn*$^{-/-}$ myocyte during exposure to 1 μM ISO. Myocytes were loaded with Fura2 AM and paced at 1 Hz (vertical lines). (*B*) Average rate of SCRs during a 20-s recording period. Note that Ca^{2+} channel block with nifedipine (NIF, 20 μM) abolished the differences between the groups. *Trdn*$^{+/+}$ (+/+): $n = 39$ (CON), 37 (ISO), and 61 (ISO + NIF); *Trdn*$^{-/-}$ (−/−): $n = 46$ (CON), 33 (ISO), and 67 (ISO + NIF); *, $P < 0.001$, Mann-Whitney test. (*C*) ECG records showing representative examples of ventricular extrasystoles (VES, #) and an episode of nonsustained ventricular tachycardia (VT) in conscious *Trdn*$^{-/-}$ mice after i.p. injection of ISO (1.5 mg/kg). (*D*) Average rate of VES and VT during a 1.5-h period after ISO challenge. *, $P < 0.05$, Mann-Whitney test. $n = 8$ mice per group.

Ryanodine pretreatment abolished the differences in I_{Ca} amplitude between the 2 groups (Fig. 3*C*), but both activation and inactivation of I_{Ca} remained significantly slower in *Trdn*$^{-/-}$ myocytes (Fig. 3*D*). Similar results were obtained in thapsigargin-treated myocytes (data not shown). Thus, although the difference in ISO-stimulated I_{Ca} amplitude can be explained by the reduced negative feedback from SR Ca^{2+} release, a component of I_{Ca} inactivation is independent of Ca^{2+} release. To test whether channel gating is altered, we used Ba^{2+} as a charge carrier, which does not trigger SR Ca^{2+} release and does not cause Ca^{2+}-dependent inactivation (19). Although not different in control conditions (data not shown), in the presence of ISO, both activation and inactivation of I_{Ba} had significantly slower kinetics in *Trdn*$^{-/-}$ compared with *Trdn*$^{+/+}$ myocytes (Fig. S2).

We next examined the consequences of triadin deletion and CRU remodeling on SR Ca^{2+} release and storage. The amplitude and rate of SR Ca^{2+} release was significantly reduced in *Trdn*$^{-/-}$ compared with *Trdn*$^{+/+}$ myocytes (Fig. 4 *A–C*). ISO abolished the differences in Ca^{2+} transient amplitude (Fig. 4 *A* and *B*), but the rate of SR Ca^{2+} release remained significantly slower in *Trdn*$^{-/-}$ compared with *Trdn*$^{+/+}$ myocytes (Fig. 4*C*). Diastolic Ca^{2+} (Fig. 4*D*) and SR Ca^{2+} content (Fig. 4 *A* and *E*) were significantly increased in *Trdn*$^{-/-}$ compared with *Trdn*$^{+/+}$ myocytes. Consistent with the decreased colocalization of Cav1.2 and RyR2 channels (Fig. 2*E*), the fraction of SR Ca^{2+} content released in response to a steady-state field stimulus (= fractional release) was significantly reduced in *Trdn*$^{-/-}$ myocytes (Fig. 4*F*). Together with the finding that I_{Ca} of *Trdn*$^{-/-}$ myocytes was not different in control conditions (Fig. 3*A*) and that it increased in the presence of ISO (Fig. 3*C*), these results demonstrate that E-C coupling efficiency is impaired in *Trdn*$^{-/-}$ myocytes.

To investigate what caused the increased SR Ca^{2+} content of *Trdn*$^{-/-}$ myocytes, we estimated SR Ca^{2+} uptake by fitting the decay of Ca^{2+} transients to a monoexponential function. Compared with *Trdn*$^{+/+}$ myocytes, the average decay time constant of *Trdn*$^{-/-}$ myocytes was significantly slower in control conditions [*tau* (s): *Trdn*$^{+/+}$: $0.175 \pm 0.005, n = 37$ vs. *Trdn*$^{-/-}$: $0.347 \pm 0.037, n = 38$; $P < 0.001$] and not significantly different during ISO challenge [*tau* (s): *Trdn*$^{+/+}$: $0.081 \pm 0.16, n = 31$ vs. *Trdn*$^{-/-}$: $0.080 \pm 0.34, n = 23$; $P = 0.89$]. NaCa exchanger function, estimated by the time constant of cytosolic Ca^{2+} decay during caffeine application was also not significantly different between the 2 groups [*tau* (s): *Trdn*$^{+/+}$: $2.02 \pm 0.14, n = 37$ vs. *Trdn*$^{-/-}$: $1.82 \pm 0.31, n = 38$; $P = 0.56$]. On the other hand, measuring SR Ca^{2+} content in unpaced, quiescent myocytes (F_{ratio}: *Trdn*$^{+/+}$ $1.35 \pm 0.10, n = 33$ vs. *Trdn*$^{-/-}$ $1.34 \pm 0.11, n = 30$; $P = 0.95$), or blocking I_{Ca} with 20 μM nifedipine (F_{ratio}: *Trdn*$^{+/+}$ $1.13 \pm 0.11, n = 17$ vs. *Trdn*$^{-/-}$ $1.15 \pm 0.11, n = 12$; $P = 0.90$) abolished the differences between the 2 groups. Taken together, these data suggest that the impaired inactivation of I_{Ca} causes excess Ca^{2+} influx, which was responsible for the increased SR Ca^{2+} content of *Trdn*$^{-/-}$ myocytes.

ISO Challenge Causes SCRs in *Trdn*$^{-/-}$ Myocytes and Ventricular Arrhythmia in *Trdn*$^{-/-}$ Mice. Myocyte Ca^{2+} overload can cause SCR, Ca^{2+} waves, and triggered beats (22). On the other hand, because triadin-1 reportedly sensitizes the CRU to luminal Ca^{2+} (7, 9), triadin-1 deletion may prevent SCR even under conditions of high SR Ca^{2+} load observed in *Trdn*$^{-/-}$ myocytes. The net effect of Ca^{2+} overload in myocytes lacking triadin was an increased incidence of SCRs during ISO exposure (Fig. 5 *A* and *B*). Conducting the ISO challenge in quiescent myocytes without field stimulation (SCR/min: *Trdn*$^{+/+}$ $13 \pm 2.8, n = 41$ vs. *Trdn*$^{-/-}$ $11.8 \pm 2.9, n = 32$; $P = 0.64$) or pretreatment with nifedipine (20 μM) abolished the differences in SCR incidence between the 2 groups (Fig. 5*B*).

We next studied global cardiac function in vivo (Table S1). *Trdn*$^{-/-}$ mice had increased cardiac contractility measured by echocardiography. Heart/body weight ratio of *Trdn*$^{-/-}$ mice was

increased by 26% ($P < 0.001$). Histologic analysis of ventricular sections did not reveal any evidence for fibrosis, inflammation, myofibrillar disarray, or myocyte hypertrophy in *Trdn*$^{-/-}$ hearts (data not shown). Electrocardiogram (ECG) evaluation demonstrated significant sinus bradycardia, increased P-wave amplitude, and widened QRS complex, but normal repolarization parameters (Table S1). Upon ISO challenge, *Trdn*$^{-/-}$ mice displayed a significantly higher rate of ventricular ectopy and nonsustained ventricular tachycardia than *Trdn*$^{+/+}$ mice (Fig. 5 *C* and *D*).

Taken together, these results suggest that the structural remodeling of the dyad coupled with myocyte Ca^{2+} overload as a result of impaired Ca^{2+}-dependent inactivation of Cav1.2 was sufficient to cause stress-induced ventricular tachycardia in *Trdn*$^{-/-}$ mice.

Discussion

Our results indicate that cardiac triadin-1 is critically important for maintaining the structural integrity of the cardiac CRU. The absence of triadin-1 leads to a loss of dyads and to a reduction in the size of T-tubule–jSR contacts. The structural abnormalities are accompanied by reduction of jSR proteins located in the dyad. The CRU remodeling significantly impaired Ca^{2+} release-dependent inactivation of Cav1.2, resulting in myocyte Ca^{2+} overload and SCR events, and ventricular arrhythmias in vivo. Although it is difficult to know which functional changes are caused directly by the absence of *Trdn* and which are consequences of secondary changes such as the CRU remodeling, our results clearly suggest that *TRDN* should be considered as a candidate gene for arrhythmia susceptibility in humans.

The mechanism that underlies the *Trdn*-linked arrhythmia phenotype is surprisingly different from that of genes associated with catecholaminergic ventricular tachycardia (11, 13). Unlike ventricular tachycardia caused by *Casq2* or *RyR2* mutations, which cause SR Ca^{2+} leak and triggered beats at normal or decreased SR Ca^{2+} load (11), deletion of triadin-1 increases the frequency of SCRs and extra beats by *increasing* SR Ca^{2+} content. We speculate that the dramatically reduced feedback inhibition of I_{Ca} by SR Ca^{2+} release caused a net increase of Ca^{2+} influx into the cell. Consistent with this hypothesis, I_{Ca} inhibition with nifedipine prevented excessive Ca^{2+} loading of the SR and the resultant SCRs. Furthermore, although not tested here, it is possible that slow inactivation of I_{Ca} contributed to the high incidence of ventricular ectopy via generation of early afterdepolarizations (23).

Our data suggest that 2 mechanisms exist whereby absence of triadin-1 impairs I_{Ca} inactivation, resulting in myocyte Ca^{2+} overload. First, the dyadic membranes within *Trdn*$^{-/-}$ cardiomyocytes exhibit an altered architecture, with a reduced colocalization of Cav1.2 with RyR2 channels according to our electron microscopy, immunolabeling, and ligand-binding results. We hypothesize that these structural changes reduce the negative feedback that SR Ca^{2+} release normally exerts on I_{ca} (19), given that most differences in I_{Ca} can be prevented by block of SR Ca^{2+} release with ryanodine or depletion of Ca^{2+} stores with thapsigargin. A second component of I_{Ca} inactivation remains insensitive to SR Ca^{2+} release inhibition and is observed even when Ba^{2+} was used as charge carrier, suggesting that Cav1.2 channel gating properties are altered independently of RyR2 activity and the filling state of SR. Interestingly, altered channel gating is only evident in ISO-stimulated *Trdn*$^{-/-}$ myocytes. It is possible that Cav1.2 channels located outside of dyads exhibit different gating properties, and/or that these channels are nonconducting unless activated by ISO. Whether disruption of a form of bidirectional signaling between Cav1.2 and RyR2 could have contributed to the differences in channel gating remains to be explored. Weak conformational coupling between these proteins has been proposed (24) but remains elusive in cardiac muscle. Other possibilities include enhanced I_{Ca} mode 2 gating (25), altered subunit composition favoring I_{Ca} facilitation (26), or CaMKII-mediated I_{Ca} facilitation (27), although intact SR Ca^{2+} release is reportedly required for the latter (27).

It has been previously shown that overexpression of triadin-1 sensitizes RyR2 channels, increases E-C coupling gain, and causes SCR (7). According to these studies, loss of triadin-1 should desensitize the SR-release complex and decrease E-C coupling efficiency. Although *Trdn*$^{-/-}$ myocytes exhibited impaired SR Ca^{2+} release, the altered jSR anatomy (50% reduction in the extent of junctional contacts between SR and T-tubules) is likely to be a major contributor. The increased rate of SCR observed here is not consistent with a primary effect of RyR2 desensitization (22) but more likely the consequence of the increased SR Ca^{2+} content observed in *Trdn*$^{-/-}$ myocytes. However, our experiments do not rule out that loss of triadin-1 desensitized the RyR2 complex (9). The concomitant reduction in Casq2 that occurs in *Trdn*$^{-/-}$ myocytes may offset any modulation of RyR2 activity imparted by the lack of triadin-1 (9, 13). The net effect on intrinsic RyR2 activity will have to be addressed by direct measurements of RyR2 function.

Triadin and junctin reportedly anchor Casq2 to RyR2 (3, 6, 28). In the presence of the 2 proteins Casq2 is restricted to the jSR cisternae and arranged in small clusters (29). The less dense configuration of Casq2 in the jSR lumen and the partial movement of Casq2 into the free SR are consistent with the drastic reduction in junctin and complete loss of triadin-1 in *Trdn*$^{-/-}$ myocytes. Overall, the structural analysis indicates a much looser association of Casq2 with the RyR2 complex. Although the functional significance of these changes remains to be explored, it may decrease the rate of Ca^{2+} diffusion within the SR lumen and thereby contribute to the slow rate of Ca^{2+} release observed in *Trdn*$^{-/-}$ myocytes. The presence of Casq2 in the free SR lumen is not easily detected in electron micrographs, probably because Casq2 concentration is relatively low and thus it does not form a gel of the type seen when Casq2 is overexpressed (30). The second effect of *Trdn* deletion, the fragmentation of the jSR cisternae and the resulting decrease in jSR–T-tubule contacts and decreased Cav1.2-RyR2 colocalization, may be the result of a decrease in junctophilin 1 and 2 rather than a direct effect of triadin absence. By partially uncoupling Cav1.2 from RyR2, this configuration change may be the one with the strongest functional effect, as discussed above. The underlying mechanism of how loss of triadin causes a reduction in the jSR proteins will have to be determined in future studies.

A recent report showed a dramatic downregulation of junctin (below level of detection) and triadin (22%) in human failing hearts (31). Downregulation of triadin-1 in human heart failure may contribute to the decreased E-C coupling efficiency observed in models of heart failure (32). Surprisingly, despite decreased Ca^{2+} transients and contractility of individual myocytes, fractional left ventricular shortening was increased in anesthetized *Trdn*$^{-/-}$ mice. Several factors likely contributed to enhanced contractility in vivo: absence of heart fibrosis and myocyte hypertrophy suggests that myocyte hyperplasia may increase the muscle mass of *Trdn*$^{-/-}$ hearts, which would offset hypocontractility at the individual myocyte level. Circulating catecholamines may further enhance contractility in vivo, considering that in individual ISO-stimulated *Trdn*$^{-/-}$ myocytes, Ca^{2+} transients and contractility were not different from wild-type myocytes. Finally, the slower heart rate of *Trdn*$^{-/-}$ mice allows increased left ventricular filling during diastole, which would increase apparent left ventricular fractional shortening regardless of intrinsic myocardial contractility (33).

We conclude that ablation of the jSR protein triadin causes susceptibility to ventricular arrhythmias in mice. The underlying mechanism for the arrhythmia phenotype seems to be the structural remodeling of the cardiac Ca^{2+} release unit, which results in

impaired E-C coupling and impaired contractility at the level of the myocyte. Although catecholamines can normalize contractile function by increasing I_{Ca} and SR Ca^{2+} content, it comes at the price of an increased risk for spontaneous Ca^{2+} releases in myocytes and triggered ventricular arrhythmias in vivo.

Methods

Animal Model. The use of animals in this study was in accordance to National Institutes of Health guidelines and approved by the Vanderbilt University Laboratory Animal Care and Use Committee. Sex-matched *Trdn*$^{+/+}$ and *Trdn*$^{-/-}$ mice, C57/black6 strain, of 4–7 months of age were used for all of the experiments.

Protein Analysis. Mouse ventricular homogenates and microsomes were prepared, immunoblotted ,and quantified as previously described (11); see also *SI Methods*.

Electron Microscopy. Hearts from 6–7-month-old *Trdn*$^{+/+}$ and *Trdn*$^{-/-}$ mice were harvested, the aorta cannulated, and hearts fixed by retrograde reperfusion with 3% glutaraldehyde in 0.1 M sodium cacodylate buffer, pH 7.2. Hearts were processed, imaged by electron microscopy, and estimates of relative surface areas and volumes of the total obtained as previously described (11), with a factor of 2 correction. Lengths and widths of the jSR cisternae profiles were measured with Photoshop (Adobe Systems). All quantitative data were obtained from 3 hearts each for *Trdn*$^{+/+}$ and *Trdn*$^{-/-}$ mice.

Heart Histology. Hearts were harvested from 6 age- and sex-matched mice per genotype, fixed, sectioned, stained, and the amount of inflammation, cell hypertrophy, myofiber disarray, and fibrosis quantified by an experienced pathologist blinded to the genotype; see also *SI Methods*.

Immunolabeling and Colocalization Experiments. Isolated ventricular myocytes were used for fixation, permeabilization, and immunolabeling, as well as processing, deconvolving, and analyzing images as previously described (34); see also *SI Methods*.

Myocyte Isolation and Ca^{2+} Fluorescence Measurements. Single ventricular myocytes were isolated, loaded with the membrane-permeable fluorescent Ca^{2+} indicator Fura-2 AM, and [Ca^{2+}] measured as previously described (11); see also *SI Methods*.

Analysis of SCRs. An SCR was defined as any spontaneous increase of 0.1 ratiometric units (3 times the average background noise) or more from the diastolic F_{ratio} other than when triggered by field stimulation or caffeine (11). For each myocyte, SCRs were counted over a 20-s period. SCRs and SR Ca^{2+} content were also analyzed in myocytes after 20-min incubation with the Cav1.2 channel blocker nifedipine 20 μM.

Voltage-Clamp Studies. Cav1.2 Ca^{2+} currents were measured as previously described (11); see also *SI Methods*.

ECG Recordings and Echocardiography. For the surface ECG and echocardiography, recordings were done as previously described (11). ISO challenge was performed on unrestrained telemetry-implanted mice as described previously (11).

Statistical Analysis. All experiments were done in random sequence with respect to the genotype, and measurements were taken by a single observer who was blinded to the genotype. Differences between groups were assessed using a one-way analysis of variance (for normally distributed parameters) or by Kruskal-Wallis test (for parameters that are not normally distributed). If statistically significant differences were found, individual groups were compared with Student's *t* test or by nonparametric tests, as indicated in the text. Results were considered statistically significant if the *P* value was <0.05. Unless otherwise indicated, results are expressed as arithmetic means $\pm$ SEM.

ACKNOWLEDGMENTS. We thank Dr. W. Catterall for the gift of CNC Cav1.2 antibody (National Institutes of Health Grant R01 HL085372); and Hyun Hwang, Izabela Holinstat, and Sergio Coffa for their technical assistance with the myocyte isolation, breeding, and genotyping of the mice. This work was supported by National Institutes of Health Grants R01 HL88635 and R01 HL71670 (to B.C.K.), R01 HL48093 (to C.F.A.), P01 AR044750 (to P.D.A., I.N.P., and C.F.A.), HL49428 (to L.R.J.), and T32 ES07059 (to R.A.C.); American Heart Association Established Investigator Award 0840071N (to B.C.K.); and Canadian Institutes of Health Research Grants MOP12875 and HSFBC&Y (to E.D.M.).

1. Flucher BE, Franzini-Armstrong C (1996) Formation of junctions involved in excitation-contraction coupling in skeletal and cardiac muscle. *Proc Natl Acad Sci USA* 93:8101–8106.
2. Bers DM (2004) Macromolecular complexes regulating cardiac ryanodine receptor function. *J Mol Cell Cardiol* 37:417–429.
3. Zhang L, Kelley J, Schmeisser G, Kobayashi YM, Jones LR (1997) Complex formation between junctin, triadin, calsequestrin, and the ryanodine receptor. Proteins of the cardiac junctional sarcoplasmic reticulum membrane. *J Biol Chem* 272:23389–23397.
4. Guo W, Jorgensen AO, Jones LR, Campbell KP (1996) Biochemical characterization and molecular cloning of cardiac triadin. *J Biol Chem* 271:458–465.
5. Caswell AH, Brandt NR, Brunschwig JP, Purkerson S (1991) Localization and partial characterization of the oligomeric disulfide-linked molecular weight 95,000 protein (triadin) which binds the ryanodine and dihydropyridine receptors in skeletal muscle triadic vesicles. *Biochemistry* 30:7507–7513.
6. Kobayashi YM, Jones LR (1999) Identification of triadin 1 as the predominant triadin isoform expressed in mammalian myocardium. *J Biol Chem* 274:28660–28668.
7. Terentyev D, et al. (2005) Triadin overexpression stimulates excitation-contraction coupling and increases predisposition to cellular arrhythmia in cardiac myocytes. *Circ Res* 96:651–658.
8. Kirchhefer U, et al. (2004) Transgenic triadin 1 overexpression alters SR Ca2+ handling and leads to a blunted contractile response to beta-adrenergic agonists. *Cardiovasc Res* 62:122–134.
9. Gyorke I, Hester N, Jones LR, Gyorke S (2004) The role of calsequestrin, triadin, and junctin in conferring cardiac ryanodine receptor responsiveness to luminal calcium. *Biophys J* 86:2121–2128.
10. Kirchhefer U, et al. (2001) Cardiac hypertrophy and impaired relaxation in transgenic mice overexpressing triadin 1. *J Biol Chem* 276:4142–4149.
11. Knollmann BC, et al. (2006) Casq2 deletion causes sarcoplasmic reticulum volume increase, premature Ca2+ release, and catecholaminergic polymorphic ventricular tachycardia. *J Clin Invest* 116:2510–2520.
12. Gyorke S, et al. (2002) Regulation of sarcoplasmic reticulum calcium release by luminal calcium in cardiac muscle. *Front Biosci* 7:d1454–d1463.
13. Chopra N, et al. (2007) Modest reductions of cardiac calsequestrin increase sarcoplasmic reticulum Ca2+ leak independent of luminal Ca2+ and trigger ventricular arrhythmias in mice. *Circ Res* 101:617–626.
14. Yuan Q, et al. (2007) Sarcoplasmic reticulum calcium overloading in junctin deficiency enhances cardiac contractility but increases ventricular automaticity. *Circulation* 115:300–309.
15. Shen X, et al. (2007) Triadins modulate intracellular Ca2+ homeostasis but are not essential for excitation-contraction coupling in skeletal muscle. *J Biol Chem* 282:37864–37874.
16. Phimister AJ, et al. (2007) Conformation-dependent stability of junctophilin 1 (JP1) and ryanodine receptor type 1 (RyR1) channel complex is mediated by their hyper-reactive thiols. *J Biol Chem* 282:8667–8677.
17. Nabauer M, Callewaert G, Cleemann L, Morad M (1989) Regulation of calcium release is gated by calcium current, not gating charge, in cardiac myocytes. *Science* 244:800–803.
18. Lee KS, Marban E, Tsien RW (1985) Inactivation of calcium channels in mammalian heart cells: Joint dependence on membrane potential and intracellular calcium. *J Physiol* 364:395–411.
19. Adachi-Akahane S, Cleemann L, Morad M (1996) Cross-signaling between L-type Ca2+ channels and ryanodine receptors in rat ventricular myocytes. *J Gen Physiol* 108:435–454.
20. Cohen NM, Lederer WJ (1988) Changes in the calcium current of rat heart ventricular myocytes during development. *J Physiol* 406:115–146.
21. Bers DM (2000) Calcium fluxes involved in control of cardiac myocyte contraction. *Circ Res* 87:275–281.
22. Venetucci LA, Trafford AW, Eisner DA (2007) Increasing ryanodine receptor open probability alone does not produce arrhythmogenic calcium waves: Threshold sarcoplasmic reticulum calcium content is required. *Circ Res* 100:105–111.
23. Wit AL, Rosen MR (1983) Pathophysiologic mechanisms of cardiac arrhythmias. *Am Heart J* 106(4 Pt 2):798–811.
24. Huang G, et al. (2007) Ca2+ signaling in microdomains: Homer1 mediates the interaction between RyR2 and Cav1.2 to regulate excitation-contraction coupling. *J Biol Chem* 282:14283–14290.
25. Hess P, Lansman JB, Tsien RW (1984) Different modes of Ca channel gating behaviour favoured by dihydropyridine Ca agonists and antagonists. *Nature* 311:538–544.
26. Dai S, Klugbauer N, Zong X, Seisenberger C, Hofmann F (1999) The role of subunit composition on prepulse facilitation of the cardiac L-type calcium channel. *FEBS Lett* 442:70–74.
27. Wu Y, Dzhura I, Colbran RJ, Anderson ME (2001) Calmodulin kinase and a calmodulin-binding 'IQ' domain facilitate L-type Ca2+ current in rabbit ventricular myocytes by a common mechanism. *J Physiol* 535(Pt 3):679–687.
28. Kobayashi YM, Alseikhan BA, Jones LR (2000) Localization and characterization of the calsequestrin-binding domain of triadin 1. Evidence for a charged beta-strand in mediating the protein-protein interaction. *J Biol Chem* 275:17639–17646.
29. Zhang L, Franzini-Armstrong C, Ramesh V, Jones LR (2001) Structural alterations in cardiac calcium release units resulting from overexpression of junctin. *J Mol Cell Cardiol* 33:233–247.
30. Tijskens P, Jones LR, Franzini-Armstrong C (2003) Junctin and calsequestrin overexpression in cardiac muscle: The role of junctin and the synthetic and delivery pathways for the two proteins. *J Mol Cell Cardiol* 35:961–974.
31. Gergs U, et al. (2007) On the role of junctin in cardiac Ca2+ handling, contractility, and heart failure. *Am J Physiol Heart Circ Physiol* 293:H728–H734.
32. Gomez AM, et al. (1997) Defective excitation-contraction coupling in experimental cardiac hypertrophy and heart failure. *Science* 276:800–806.
33. Nemoto S, DeFreitas G, Mann DL, Carabello BA (2002) Effects of changes in left ventricular contractility on indexes of contractility in mice. *Am J Physiol Heart Circ Physiol* 283:H2504–H2510.
34. Scriven DR, Klimek A, Asghari P, Bellve K, Moore ED (2005) Caveolin-3 is adjacent to a group of extradyadic ryanodine receptors. *Biophys J* 89:1893–1901.